IOPscience iopscience.iop.org

Home Search Collections Journals About Contact us My IOPscience

The interface roughness exponent in Ge_xSi_{1-x}/Si superlattices

This article has been downloaded from IOPscience. Please scroll down to see the full text article.

1997 J. Phys.: Condens. Matter 9 2891

(http://iopscience.iop.org/0953-8984/9/14/005)

View the table of contents for this issue, or go to the journal homepage for more

Download details:
IP Address: 171.66.16.151
The article was downloaded on 12/05/2010 at 23:07

Please note that terms and conditions apply.

J. Phys.: Condens. Matter **9** (1997) 2891–2902. Printed in the UK PII: S0953-8984(97)74280-2

The interface roughness exponent in Ge_xSi_{1-x}/Si superlattices

S F Cui†, G M Luo†, M Li†, Z H Mai†, Q Cui†, J M Zhou†, X M Jiang‡ and W L Zhang‡

† Institute of Physics, Chinese Academy of Sciences, Beijing 100080, People's Republic of China

‡ Institute of High Energy Physics, Chinese Academy of Sciences, Beijing 100039, People's Republic of China

Received 7 May 1996, in final form 23 September 1996

Abstract. The interface roughness and scaling exponent of Ge_xSi_{1-x}/Si strained-layer superlattices (SLSs) grown by molecular beam epitaxy (MBE) have been measured by x-ray reflectivity and diffuse-scattering methods. We have found that for samples grown under identical conditions the root mean square (rms) roughnesses (σ), the roughness exponents (h), and the lateral correlation length (ξ) are dependent upon the thickness and/or the substrate temperatures of the superlattice. The incorporation of a surfactant, such as antimony, can retard interface widening and smooth the interface.

1. Introduction

Recently there has been considerable interest in the properties of epitaxially grown strained-layer superlattices (SLSs) of Ge_xSi_{1-x}/Si due to their potentially important applications in various optoelectronic and microelectronic devices [1]. Since the quality of interfaces can greatly influence the strain and electron transport in thin-layer heterostructures [2, 3], it is necessary to achieve a detailed knowledge of the interface microstructures of layered materials. It has been shown by numerous theoretical and experimental studies that the scattering of x-rays and neutrons from rough surfaces can be divided into specular-reflection and diffuse-scattering terms, which can be calculated within the first Born approximation for weak scattering or in the distorted-wave Born approximation for intense scattering (e.g. near the critical angle for total external reflection) [4–7]. The surface roughness can be described as self-affine over finite length scales by Mandelbrot in terms of fractional Brownian motion [8]. For many isotropic solid surfaces we may write as the height–height correlation [4]

$$G(r) = \langle [z(r) - z(0)]^2 \rangle = Ar^{2h} \qquad (0 < h < 1) \tag{1}$$

where $z(r)$ is a height on the surface and $r = (x^2 + y^2)^{1/2}$. The exponent, h, determines the texture of the surface in $3 - h$ dimensions. In practical calculations we use the correlation functions of the form

$$G(r) = \sigma^2 \exp[-(r/\xi)^{2h}] \tag{2}$$

where σ is the root mean square (rms) roughness and ξ is an upper cut-off.

Equation (2) provides a method for determining the roughness exponents from x-ray diffuse-scattering experiments. Very recently, some authors [9, 10] have recognized that

0953-8984/97/142891+12$19.50 © 1997 IOP Publishing Ltd

the exponent h can spatially characterize the dynamical scaling behaviour of the growth of surfaces and interfaces [11, 12]. Models developed to describe growth processes may be divided into two categories [9, 12]: conservative growth and non-conservative growth. The first mode may be suitable for a growth process with efficient surface diffusion in which the values of the roughness exponent h in $d = 2 + 1$ dimensions are within the range $h = 2/3$ to $h = 0.95$. In the second mode, the values of the exponent h in $d = 2+1$ dimension may be close to the value $h = 1/2$ predicted by Kardar–Parisi–Zhang (KPZ) equations [12, 13].

In this paper we examine the interface roughness and the roughness exponent of Ge_xSi_{1-x}/Si SLSs grown by MBE under varying growth conditions, by means of x-ray reflectivity and diffuse scattering. We prepared samples with different thicknesses of the period of the SLSs, and grew samples with different substrate temperatures. Recently it has been reported that use of a surface surfactant can help in achieving sharp interfaces [14], and so we compare the interface morphology between samples with and without a surfactant. We found that for samples grown under identical conditions the interface roughness and/or the scaling exponents of Ge_xSi_{1-x}/Si SLSs are sensitive to the sample thicknesses and the temperatures of the substrates. The surfactant can modify the interface morphology and improve its quality. A brief explanation is proposed for our experimental results, in which the growth modes recently developed are considered. We have determined the roughness exponent h to be 0.35 to 0.5 for thick samples in which the thickness of the Ge_xSi_{1-x} component was about 95 Å and to be 0.63 to 0.7 for thin samples in which the thickness of the Ge_xSi_{1-x} component was about 46 Å. The above results indicate that the growth mode for Ge_xSi_{1-x}/Si SLSs can be modified by changing their structural parameters.

Table 1. The nominal structures of Ge_xSi_{1-x}/Si samples.

Sample	x	t_1 (Å)[a]	t_2 (Å)[b]	t_{cap} (Å)[c]	N[d]	Surfactant	T_{sub} (°C)[e]
A	0.2	240	80	0	15	—	650
B	0.2	240	80	0	15	Sb	650
C	0.2	120	40	0	15	—	650
D	0.2	120	40	0	15	Sb	650
E	0.35	320	80	1000	10	—	600
F	0.35	320	80	1000	10	—	670
G	0.35	320	80	1000	10	—	750

[a] t_1: thicknesses of Si layers in superlattice periods.
[b] t_2: thicknesses of Ge_xSi_{1-x}/Si layers in superlattice periods.
[c] t_{cap}: thicknesses of capping layers.
[d] N: period numbers.
[e] T_{sub}: temperatures of substrates.

Our paper is constructed as follows. In section 2 we describe the sample preparations and the x-ray experiments performed using synchrotron radiations. The theory for x-ray reflectivity and diffuse scattering is outlined in section 3. We report and discuss the experimental and calculated results in detail in section 4, and give our conclusions in section 5.

2. Experiment

The samples of Ge_xSi_{1-x}/Si SLSs used in the experiments were grown on silicon (001) substrates by MBE. The nominal structures of the seven samples considered here are listed in table 1. Samples A and B are, as a group of thick samples, compared with another group

of thin samples (samples C and D); within each group the samples with and/or without surfactant are also compared. During the growth of samples B and D, antimony (Sb) was selected as the surfactant. After growth of a 1000 Å silicon buffer layer, antimony was deposited on the growing surface up to 0.75 of a monolayer, and then the Ge_xSi_{1-x}/Si bilayers were deposited alternately using a conventional MBE method. Samples A and C were grown without the use of surfactant.

The reflectivity and diffuse-scattering experiments were performed at the diffuse-scattering station of the 4W1C beam line of the Beijing Synchrotron Radiation Facility (BSRF). The beam divergency was 1.0 mrad horizontally and 0.1 mrad vertically. Monochromatic radiation of wavelength 1.54 Å was selected from a triangular bent silicon crystal which was also used as a horizontal-focusing element, placed before a reflecting mirror which was a vertical-focusing element. The intensity of the x-ray beam was 1.6×10^8 counts s^{-1} and its energy resolution was 4.4×10^{-4}. The x-ray beam was confined by slits to be of size 0.2 mm vertically and 0.5 mm horizontally during the experiment.

Specular-reflectivity (θ–2θ) scans, longitudinal (θ–2θ offset) scans and transverse (ω–2θ) scans were performed using a Huber five-circle diffractometer, whose 2θ angular accuracy is nine arcseconds. The miscut angle of the substrate, if it exists, was set in the scattering plane.

Assuming z be the direction normal to the sample surface and x to be parallel to the surface plane and aligned with scattering plane, the scattering vector was calculated from [1]

$$q_x = K(\cos\beta - \cos\alpha) \qquad q_z = K(\sin\beta + \sin\alpha) \tag{3}$$

where $K = 2\pi/\lambda$ is the wave vector of the radiation in vacuum, and α and β are the angles of incidence and scattering with respect to the sample surface, respectively.

3. Theory

The specular reflection was calculated by the recursive application of the optic theory matrix method [15] which has been described elsewhere [16]. For the non-specular diffuse scattering from interfaces, the appropriate tool is the distorted-wave Born approximation (DWBA) [4–7]. For many systems prepared by sputtering, evaporation and MBE, an imperfection of one layer is transferred to the layers above [7]. For this reason in our calculations we followed the scattering formulas of Holý and Baumbach [6] in which the effect of vertical correlations between the interfaces has been included. In the model of Holý the rms roughness of the jth interface is

$$\sigma_j = [\sigma_N^2 + (N - j)\sigma_p^2]^{1/2} \tag{4}$$

where N is the number of interfaces. The interface roughness grows towards the free surface. The form for the correlations of roughnesses between the jth and kth interfaces is

$$G_{jk}(r) = \{\sigma_N^2 + [N - \max(j,k)]\sigma_p^2\} e^{-(r/\xi)^{2h}} e^{-|z_j - z_k|/\xi_{\perp,jk}} \tag{5}$$

where σ_N is the rms roughness of the substrate surface, z_i is the position of the ith interface, $\xi_{\perp,jk}$ is the vertical correlation length, and σ_p is the rms deviation of the probability distribution of the layer thicknesses.

4. Results and discussion

During the longitudinal scans the offset angles were chosen so as to make the scans far enough away from the specular-reflection rod in reciprocal space that the intensity curves

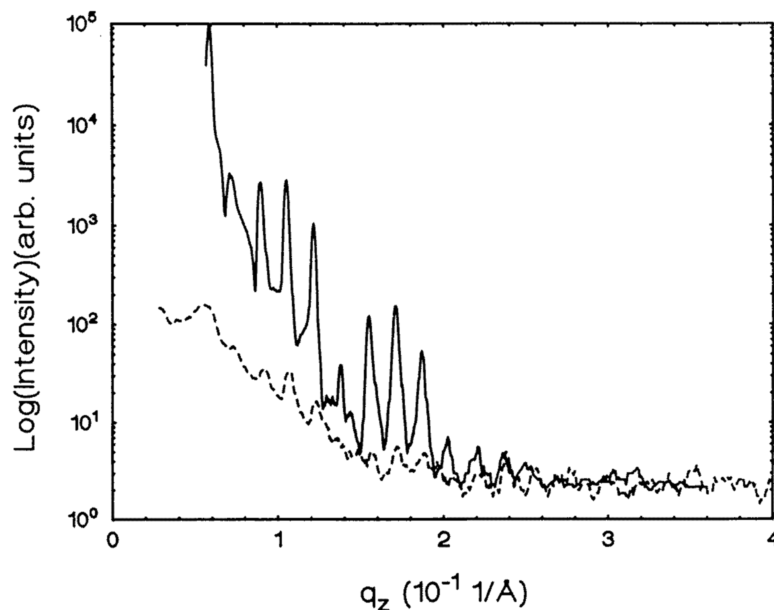

Figure 1. The specular-reflection scan (solid line) and the longitudinal diffuse scan (offset angle $\delta = 0.4°$) (dashed line) of sample B.

must be attributed to the diffuse scattering. Figure 1 shows the specular reflection and the longitudinal scattering for sample B. The Bragg peaks can be seen not only in the specular-reflection curve (upper) but also in the diffuse-scattering curve (below). This may be evidence for a vertically replicated interface structure, i.e. if the interface roughness correlates from interface to interface vertically, the diffuse scattering will exhibit Bragg resonant features when q_z matches a reciprocal-lattice spacing of the superlattice.

The true specular reflectivity of the samples was obtained by subtracting the longitudinal diffuse-scattering contributions from the specular-reflection scans [1]. In our experience this step is not necessary because the diffuse-scattering background is usually very low and does not change the shape of the specular-reflectivity curve. The amplitudes of the interference fringes seen on the reflectivity curves are determined by the interface roughness. Initially, the superlattice period was determined from the peak separation; once the period was known the individual layer thickness and the interface width were fitted to the experimental data using the matrix method [16].

Table 2. The interface roughnesses of $Ge_{0.2}Si_{0.8}/Si$ SLSs.

Sample	t_1 (Å)	t_2 (Å)	Surfactant	σ_{btm} (Å)	σ_{top} (Å)	$h(\alpha)$	ξ (Å)
A	300 ± 2	97 ± 2	—	$8(6) \pm 1$	$30(21) \pm 2$	0.35 ± 0.04	260 ± 50
B	282 ± 2	93 ± 2	Sb	6 ± 1	$23(18) \pm 2$	0.52 ± 0.04	600 ± 50
C	149 ± 2	46 ± 2	—	5 ± 1	15 ± 2	0.63 ± 0.04	2850 ± 100
D	147 ± 2	46 ± 2	Sb	5 ± 1	11 ± 2	0.7 ± 0.04	2800 ± 100

Figures 2 and 3 show the reflectivities of the two thick samples and the two thin samples, respectively. The calculated curves are in fairly good agreement with the experimental data

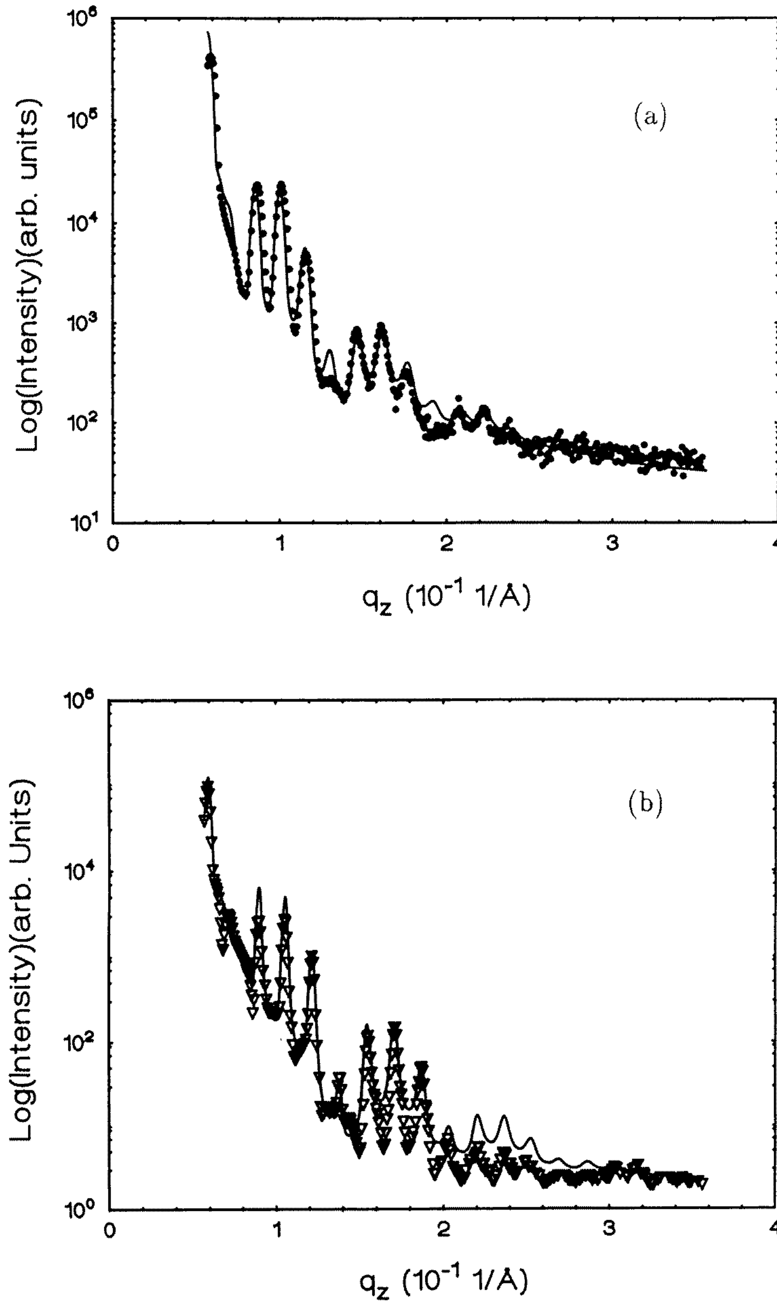

Figure 2. The reflectivity for thick samples, (a) sample A: (●) experimental; (–) calculated; (b) sample B: (▽) experimental; (–) calculated.

although discrepancies are found within a q_z-range of 0.2 to 0.3; these are believed to be due to some undesirable beam current conditions of the synchrotron radiation. From the fits to figures 2 and 3, the true structures and rms interface roughness σ for samples A, B, C,

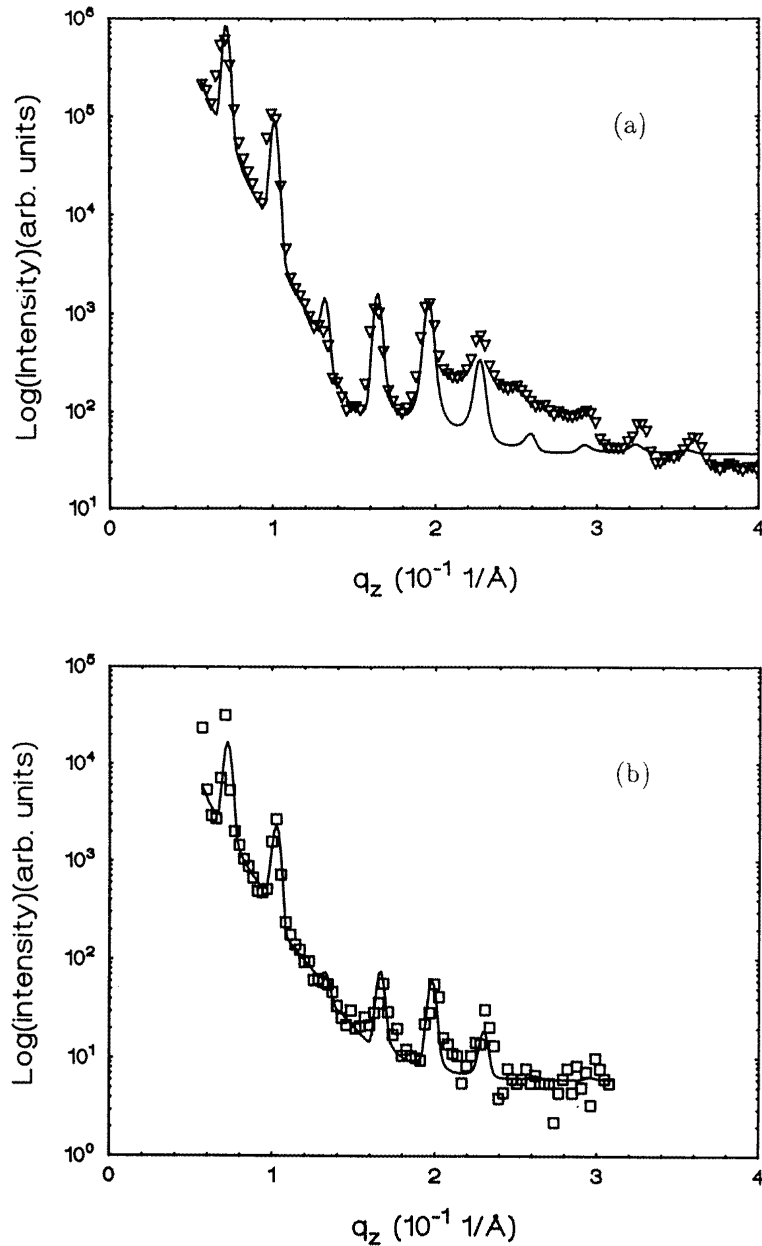

Figure 3. The reflectivity for thin samples, (a) sample C: (▽) experimental; (–) calculated; (b) sample D: (□) experimental; (–) calculated.

and D were deduced; these are listed in table 2. According to our samples having vertically replicated interface structures as mentioned above, we assume that the interface roughness grows (see section 3), so that σ_{btm} and σ_{top} represent the initial (bottom) and final (top) interface roughness of a SLS, respectively.

Figures 4 and 5 give the scans transverse to the third Bragg peaks in the reflectivity

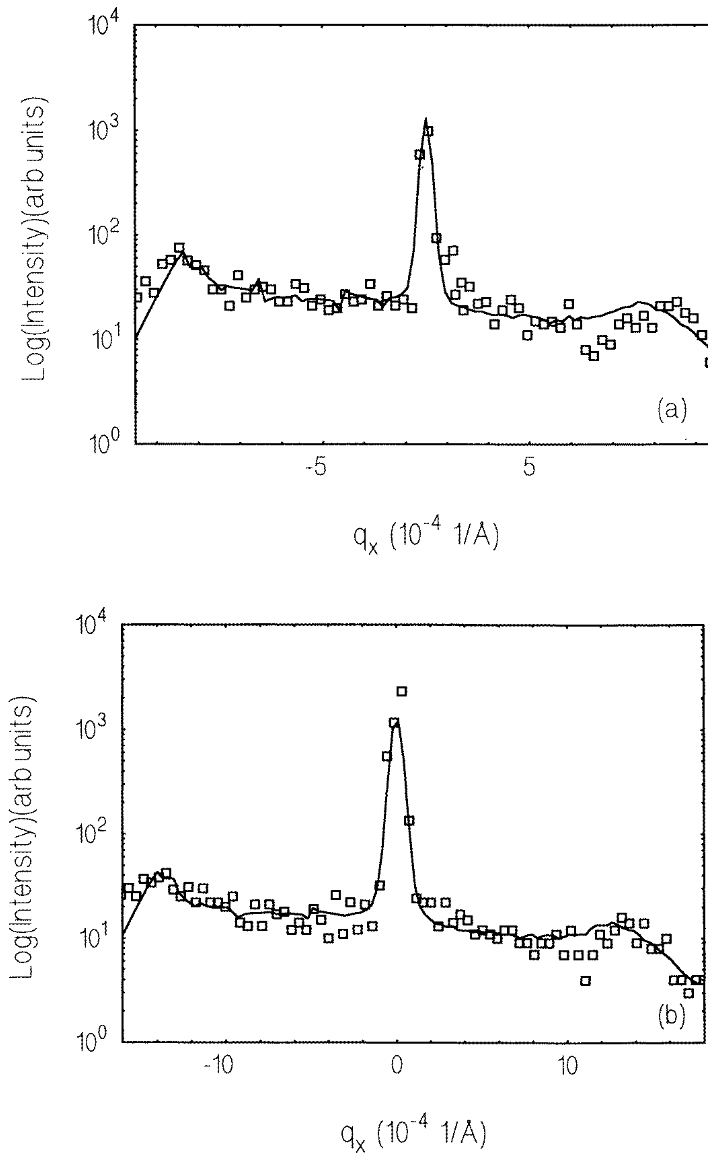

Figure 4. The scans transverse to the third-order Bragg diffraction peaks for thick samples, (a) sample A (at fixed $q_z = 0.114$ Å^{-1}); (b) sample B (at fixed $q_z = 0.122$ Å^{-1}): (□) experimental; (–) calculated.

curves (figures 2 and 3) for the above four samples. A transverse scan (along q_x, say) is characterized by a Bragg peak dominated by the resolution function, diffuse scattering, and a pair of Yoneda scattering peaks whenever the scan reaches the critical angle θ_c for total external reflection. Our experimental data display all of these features. Despite the experimental scatter due in part to the lower beam current of the synchrotron radiation, the calculated curves are in fairly good agreement with the experimental ones. From fitting to the experimental curves we obtained the roughness exponents h and the lateral correlation

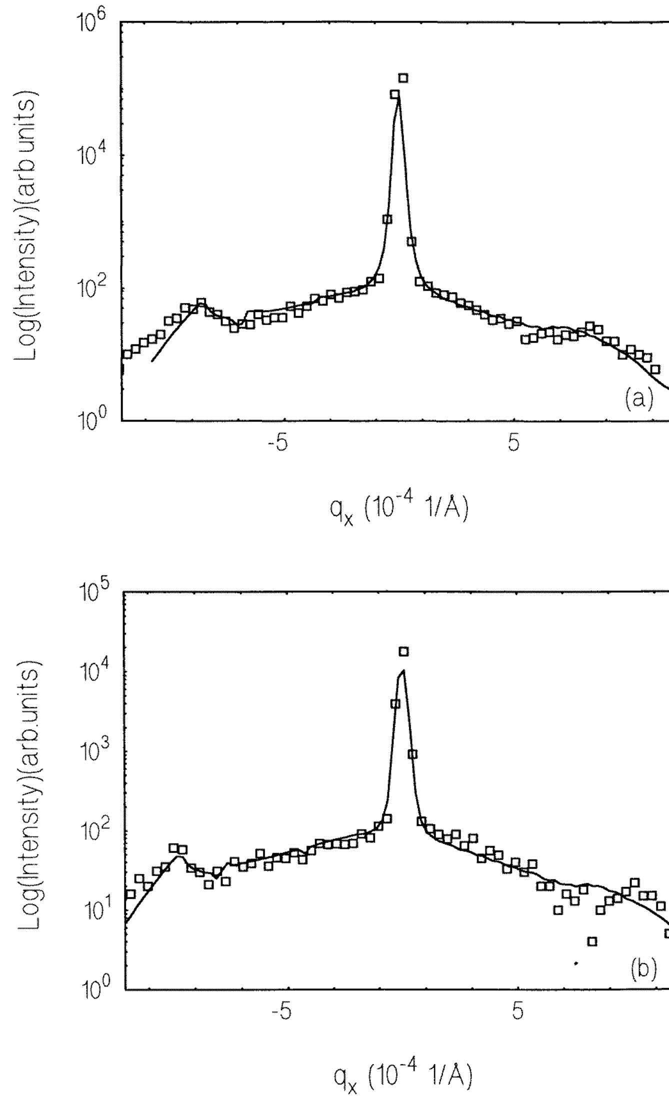

Figure 5. The scans transverse to the third-order Bragg diffraction peaks for thick samples, (a) sample C (at fixed $q_z = 0.101$ Å^{-1}); (b) sample D (at fixed $q_z = 0.108$ Å^{-1}): (□) experimental; (–) calculated.

lengths ξ for samples A, B, C, and D, which are listed in table 2. The rms roughnesses which were deduced from fitting to the transverse scan curves are given in parentheses in table 2 if they differ from those obtained from fitting to the reflectivity curves.

In the transverse scans q_z is about 0.1. For the samples C, D, E, and F the condition $|q_z\sigma|^2 \leqslant 1$ is fairly well satisfied, which is often thought of as the range of validity of the DWBA. For the samples A, B, and G, its values are out of this range by no more than a factor of four. The measurements and the calculations of the present work and of others [7] may indicate that this range is much larger.

In the work of Schlomka *et al* [7] a vertical correlation length $\xi_\perp$ is included in

the correlation functions $G_{jk}(r)$. In our calculations of the transverse scans, the vertical correlation length, $\xi_\perp$, was larger than the total thicknesses of the SLSs. For nearly perfect correlations $\xi_\perp$ is much larger than the layer thicknesses and the exponent term ($e^{-|z_j - z_k|/\xi_{\perp,jk}}$) [7] may be omitted. This shows strong vertical correlation of the interfaces for the present samples.

4.1. The effect of layer thickness on interface roughness

From table 2 one can see that for Ge_xSi_{1-x}/Si SLSs prepared under identical conditions the interface roughness, σ, increases, while the roughness exponents, h, and the lateral correlation length, ξ, decrease, with increasing sample thickness (comparing sample A with C and sample B with D in table 2).

The fact that the interface roughness increases with sample thickness can be understood according to the scaling theory of surface growth where the interface width is a measure of the correlations along the direction of growth, and grows with time [12]. On the other hand, the value of h (see the h-values of samples A and B in table 2) for thick samples is close to the value of 1/2 that is predicted by the Langevin equation [12] or more generally the KPZ equation [13] for deposition processes. This value of h corresponds to growth with only a weak relaxation, i.e. a non-conservative growth mode.

The values of h for thin samples (see the h-values of samples C and D in table 2) are 0.63–0.7, corresponding to a growth with stronger relaxation, i.e. a conservative growth mode. Given that the roughness exponent changes with the growth time we can assume that the relaxation behaviour underwent changes during growth; that is, initially the smoothing effect of surface diffusion is efficient, but later during growth this effect lessens. We believe that for a certain growth process there exists a critical time (or sample thickness) after which the system will reach a saturation state where the interface width will reach its maximum value, while the roughness exponent and upper cut-off will reach their minimum values and these values must be dependent on the particular growth conditions. In fact Rao *et al* have reported [17] that the surface width and roughness exponent change during growth and have saturation values with varying sample thickness for vapour-deposited silver films, although the situation and consequently the results are different to those of the present study. Another example is that the rms surface roughness, σ, increases with film thickness, τ, as σ is similar to τ, for plasma–polymer films revealed by atomic force microscopy [19]. The higher value of the scaling exponent may be suggestive of a layered (two-dimensional) type of growth for those thickness ranges where the exponent h is close to the predicted one for continuum deposition with the surface relaxation (CDSR) mode [18] which predicts $h = 0.67$. On the other hand, exceeding a certain thickness the growth mode might be of an island type. The island growth here results from the segregation of Ge atoms, which occurs in the GeSi layers, so one may expect that GeSi layers contribute more to the interface roughness, compared with Si layers.

4.2. The effect of surfactant on interface roughness

From table 2 one can see that the samples grown with the surfactant Sb have improved interface morphology both as regards the rms roughness and as regards in the roughness exponent, h. The role of surfactants (surface-active species) in heteroepitaxial crystal growth has been reported by some authors [14, 20]. The use of a segregating surfactant can reduce the surface free energies of the bilayers and suppress island formation. The group V elements (such as Sb as used in this paper) contain one extra valence electron per surface atom; this

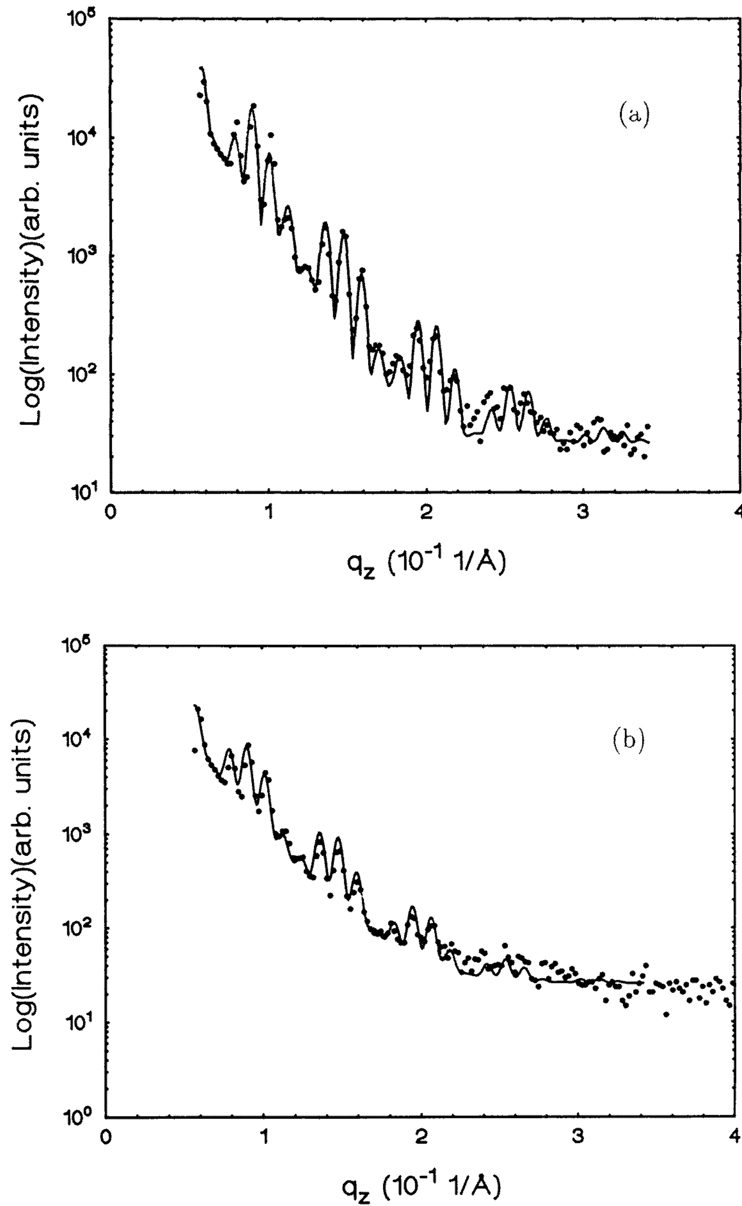

Figure 6. The reflectivity for sample E (a), sample F (b), and sample G (c): (●) experimental; (–) calculated.

fills the dangling bonds which normally occur on the clean Si(001) and Ge(001) surfaces, thereby creating a stable termination. By using the Sb-passivated surface as a stage of MBE growth, we are able to alter the growth mode of an epitaxial layer to induce wetting of the substrate. This leads to a large decrease in both the islanding and the interdiffusion between Si and GeSi layers. It has been shown in table 2 that the interface roughness of the top layer, σ_{top}, decreases from 21 Å to 18 Å, and that the scaling exponent h increases from

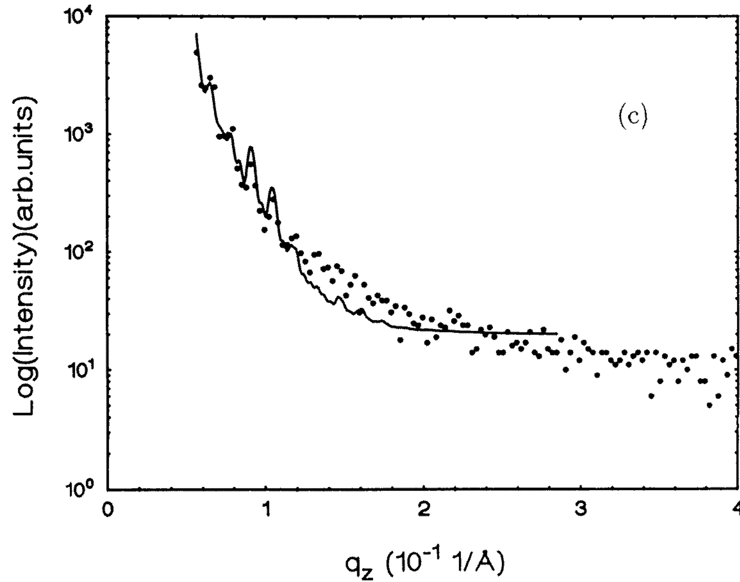

Figure 6. (Continued)

0.35 to 0.53 for thick samples, while σ_{top} decreases from 15 Å to 11 Å and h increases from 0.63 to 0.7 for thin layers. Our experimental results therefore support the arguments described above.

Table 3. The interface roughness of $Ge_{0.35}Si_{0.65}/Si$ SLSs.

Sample	t_1 (Å)	t_2 (Å)	σ_{btm} (Å)	σ_{top} (Å)	σ_{cap} (Å)	T_{sub} (°C)
E	416 ± 2	109 ± 2	4 ± 1	8 ± 2	7.6 ± 1	600
F	413 ± 2	111 ± 2	4.5 ± 1	9 ± 2	7 ± 1	670
G	339 ± 4	110 ± 4	11 ± 2	24 ± 4	12 ± 2	750

4.3. The effect of substrate temperature on interface roughness

Figures 6(a), 6(b), and 6(c) show the reflectivities of samples E, F, and G grown at substrate temperatures of 600 °C, 670 °C, and 750 °C, respectively. From fitting to the experimental data, the true structures and rms roughnesses for these samples are deduced and listed in table 3. It is worthwhile to notice that the interface roughness increased a little (8 Å to 9 Å) when the temperature of the substrates rose from 600 °C to 670 °C. On the other hand, the interface roughness increased dramatically (9 Å to 24 Å) when the temperature of the substrates rose from 670 °C to 750 °C. It needs pointing out that the larger increase of the interface width is accompanied by the decrease of the Si layers within the bilayers (from about 410 Å to 340 Å). The calculations of the reflectivities are based on a model of a Gaussian distribution of the gradient of the electronic density across the interfaces which cannot distinguish between the 'hill and valley' structures of the self-affine surface and the interdiffusion of Ge atoms. But the fact that the increase of the interface width is

accompanied by the decrease of the widths of the Si layers suggests the interdiffusion of Ge atoms to Si layers. This can be used as the criterion for distinguishing interdiffusion from true interface roughness.

On the basis of the results obtained by changing the substrate temperature, it appears that a too-high temperature of the substrate will result in interdiffusion of the bilayers of the SLSs. An optimum temperature range should thus be chosen to achieve the desired interfaces.

5. Conclusion

The interface roughness and roughness exponents of Ge_xSi_{1-x}/Si SLSs grown by MBE with varying growth conditions have been investigated using x-ray reflectivity and diffuse scattering. We have found that for samples grown under the same conditions the interface roughness and roughness exponent are dependent on the thickness of a SLS, i.e. the rms roughness σ increases, while the scaling exponent h and the lateral correlation length ξ decrease, with increasing thickness. The above results indicate that the mode of the growth can be modified by varying the structural parameters of the SLSs. The incorporation of a surfactant such as antimony (Sb) in the initial stages of growth leads to a considerably improved interface quality. We have also found that increasing the substrate temperature up to a high value causes interdiffusion of the bilayers, so care must be taken to avoid interdiffusion.

Acknowledgments

This work was supported by the National Science Foundation of China and Beijing Electron Positron Collider National Laboratory. We would like to thank Dr L S Xiu of the BSRF for assistance in the experiments. Dr P D Hatton is thanked for editing the manuscript.

References

[1] Ming Z H, Krol A, Soo Y L, Kao Y H, Park J S and Wang K L 1993 *Phys. Rev.* B **47** 16 373
[2] Osbourn G C 1984 *J. Vac. Sci. Technol.* B **2** 176
[3] Bolognesi C R, Kroemer H and English J H 1992 *Appl. Phys. Lett.* **61** 213
[4] Sinha S K, Sirota E B, Garoff S and Stanley H B 1988 *Phys. Rev.* B **38** 2297
[5] Holý V, Kubēna J, Ohlídal I, Lischka K and Plotz W 1993 *Phys. Rev.* B **47** 15 896
[6] Holý V and Baumbach T 1994 *Phys. Rev.* B **49** 10 668
[7] Schlomka J-P, Tolan M, Schwalowsky L, Seek O H, Stettner J and Press W 1995 *Phys. Rev.* B **51** 2311
[8] Mandelbrot B B 1982 *The Fractal Geometry of Nature* (New York: Freeman)
[9] Swaddling P P, McMorrow D F, Cowley R A, Ward R C C and Wells M R 1994 *Phys. Rev. Lett.* **73** 2232
[10] Salditt T, Metzger T H and Peisl J 1994 *Phys. Rev. Lett.* **73** 2228
[11] Family F and Vicsek T 1985 *J. Phys. A: Math. Gen.* **18** L75
[12] Family F 1990 *Physica* A **168** 561
[13] Kardar M, Parisi G and Zhang Y 1986 *Phys. Rev. Lett.* **56** 889
[14] Copel M, Reuter M C, Kaxiras E and Tromp R M 1989 *Phys. Rev. Lett.* **63** 632
[15] Parrat G 1954 *Phys. Rev.* **95** 359
[16] Cui S F, Li J H, Li M, Li C R, Gu Y S, Mai Z H, Wang Y T and Zhang Y 1994 *J. Appl. Phys.* **76** 4154
[17] Rao M V H, Mathur B K and Chopra K L 1994 *Appl. Phys. Lett.* **65** 124
[18] Collins G W, Letts S A, Fearon E M, McEachern R L and Bernat T P 1994 *Phys. Rev. Lett.* **73** 708
[19] Lai Z W and Das Sarma S 1991 *Phys. Rev. Lett.* **66** 2348
[20] Uhrberg R I G, Bringans R D, Bachrach R Z and Northrup J E 1986 *Phys. Rev. Lett.* **56** 520